Modeling of Polymer Erosion in Three Dimensions: Rotationally Symmetric Devices

Achim Göpferich
Dept. of Pharmaceutical Technology, University of Erlangen-Nürnberg, Cauerstrasse 4, 91058 Erlangen, Germany
and
Dept. of Chemical Engineering, Massachusetts Institute of Technology, Building E25, Room 342, Cambridge, MA 02139

Robert Langer
Dept. of Chemical Engineering, Massachusetts Institute of Technology, Building E25, Room 342, Cambridge, MA 02139

A three-dimensional erosion model was developed to simulate the erosion of polymer cylinders. Erosion is regarded as a random event. After contact with the erosion medium small polymer parts are randomly assigned lifetimes from a first-order Erlang distribution using a Monte Carlo sampling technique. The model takes into account the partially crystalline nature of polymers as well as the geometry of the devices. It allows investigation of the effect of slow or nonerodible coatings. It was found that by partially coating cylinders, erosion periods of polyanhydride polymers can be expanded substantially. This is very important for using polyanhydrides as drug carriers where the polymer erosion period controls drug release.

Introduction

Modern medicine has profited in numerous ways from the use of polymers. Applications range from the manufacture of orthopedic implants to dental material for filling cavities. For all these applications the stability of polymers is vital. The cleavage of polymer chains, *degradation*, as well as the subsequent loss of mass, *erosion*, are highly undesirable. There are, however, some special applications where polymers are meant to degrade and erode. A well-known example is surgical suture material for use inside the body, which degrades in the course of the wound healing process (Herrmann et al., 1970). During the last two decades other applications for bioerodible polymers emerged, such as drug delivery (Langer and Peppas, 1983; Göpferich et al., 1994), drug targeting to specific cells (Langer, 1990), and tissue engineering where transplantable organ tissue is grown on polymer *in vitro* followed by *in vivo* transplantation (Langer and Vacanti, 1993). Polymers that have been used for such applications include poly(orthoesters) (Heller, 1994), polyanhydrides (Rosen et al., 1983), poly(lactic acid) and poly(lactic-*co*-glycolic acid) (Wise et al., 1979). The erosion behavior of these materials is a crucial factor in device performance. All bioerodible polymers have characteristic times for erosion. Poly(lactides), for example, are stable for months, whereas some poly(orthoesters) erode in a period of weeks. For drug delivery, polyanhydrides are promising carrier materials that erode, compared to other bioerodible polymers, in a relatively short time (Rosen et al., 1988). Their advantage compared to that of most other materials is that drug delivery is primarily controlled by erosion (Göpferich and Langer, 1993a). This permits a theoretical description of erosion (Göpferich and Langer, 1993b) and the prediction of monomer and drug release (Göpferich and Langer, 1995a). Our goal was twofold: First we wanted to take advantage of the properties of polyanhydrides for long-term medication using implants. We therefore wanted to expand the drug release periods of polyanhydrides by partially coating polyanhydride matrix discs. Secondly we wanted to extend existing erosion models to allow for the description of erosion in three dimensions.

Correspondence concerning this article should be addressed to A. Göpferich.
This article is dedicated to Dr. Werner Pfaffe.

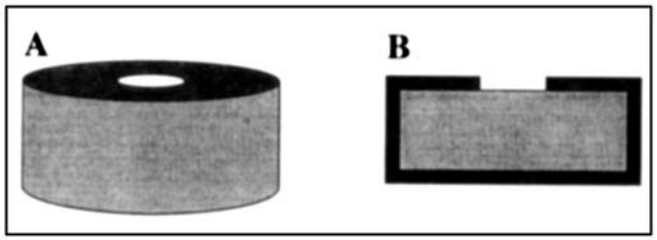

Figure 1. Coated cylinders.

(a) Three-dimensional image. (b) Cross section.

To achieve these goals we first developed an erosion model that allows predicting the erosion of polyanhydride cylinders before and after coating. As drug release periods are correlated with erosion periods simulations with such models can be used to investigate the effect of coating on drug release. For testing the quality of model predictions, the release of brilliant blue, a low molecular weight hydrophilic drug was investigated. Brilliant blue is trapped inside the polymer and owing to its hydrophilic nature, it is released immediately upon erosion. The degree of agreement between predicted erosion and drug release can be taken as a quality criterion for the model.

After assessing the impact of coating on erosion via modeling, we wanted to establish the benefit of coating experimentally using indometacin as a model drug. Polymer matrix cylinders made of poly(1,3-bis-*p*-carboxyphenoxypropane-*co*-sebacic acid), *p*(CPP-SA) and poly(fatty acid dimer-*co*-sebacic acid), *p*(FAD-SA), were partially coated using nondegradable materials like poly(ethylene-*co*-vinyl acetate), EVAc, or slowly eroding biodegradable polymers like poly(D,L-lactic acid), D,L-PLA. Just a small orifice on top of the cylinders was noncoated, as shown in Figure 1.

Materials and Methods

Materials

Indomethacin was purchased from Sigma Chemical Company, St. Louis, MO. Brilliant blue was purchased from Fluka, Buchs, Switzerland. Poly(D,L-lactic acid), D,L-PLA, was donated by Boehringer Ingelheim, Ingelheim, Germany, poly(1,3-bis-*p*-carboxyphenoxypropane-*co*-sebacic acid), *p*(CPP-SA) 50:50, *p*(CPP-SA) 20:80, and poly(fatty acid dimer-*co*-sebacic acid), *p*(FAD-SA) 50:50, were donated by Scios-Nova Pharmaceuticals, Baltimore, MD, poly(ethylene-*co*-vinyl acetate) (EVAc: 40% w/w vinyl acetate, Elvax 40W), was donated by Dupont, Wilmington, DE and purified as described in Langer (1981).

Methods

Preparation of Polymer Discs and Coatings. For the investigation of polymer erosion, discs of 8 mm diameter and 1 mm thickness were prepared by a melt casting method (Tamada and Langer, 1992). The polymer was melted at 100°C in an achat mortar, and the appropriate amount of indomethacin or brilliant blue was dissolved therein. For partial coating, the cylindric polymer matrix discs were mounted on a 3-mm teflon rod by pressing the 140°C hot rod into the center of the discs and cooling them down to room temperature in a desiccator. The matrices were then coated by simply dipping them into a 10% solution of the appropriate coating polymer dissolved in methylene chloride.

Erosion Experiment. The polymer matrix discs were eroded in 10 mL, 0.1 M phosphate buffer, pH 7.4, under gentle shaking (60 rpm) at 37°C. The buffer was changed at least daily to maintain sink conditions and was analyzed for released indomethacin or brilliant blue. The drug and dye concentrations in the acceptor were thus always kept below 10% of the solubility.

Determination of Indomethacin Release by HPLC. The release of indomethacin was determined by HPLC. A Waters HPLC (high-performance liquid chromatography) setup was used comprising two M510 pumps, a M490 UV detector, and a Wisp 712 autosampler, from Millipore, Bedford, MA. As stationary phase we used a PRP-1 Hamilton column 4.1×150 mm with 5-μm particles from Rainin Instruments, Woburn, MA. The mobile phase was a mixture of 900 mL acetonitrile, 300 mL water, and 2 mL, 1 M HCl. The flow rate was 1.2 mL/min. Peaks were detected at 246 nm. The retention time under these conditions was 6 min.

Calculations and Simulations. All algorithms for simulations and calculations were programmed in Pascal. Programs were run on a Macintosh IIsi from Apple Computer Inc., Cupertino, CA, using a Pascal compiler from Symantec, Cupertino, CA.

Results and Discussion

Erosion modeling

We applied an algorithm originally developed to describe the erosion of partially crystalline polymers in two dimensions (Göpferich and Langer, 1993b). Similar models were used to simulate the erosion of composite materials consisting of a compressed mixture of filler and drug (Zygourakis, 1990). In our previous approach polymer matrix cross sections were covered with a two-dimensional rectangular computational grid. Each created pixel represented either an amorphous or a crystalline part of the polymer matrix. The erosion of these "polymer pixels" was assumed to depend on two features: the contact of a pixel with the degradation medium, and its crystalline or amorphous nature. Just as the polymer is assumed to erode exclusively by hydrolysis, pixels not in contact with water will not erode. Pixels on the surface of the polymer matrix or next to an eroded neighbor have contact to water and therefore have the chance to erode. Crystalline matrix parts erode slower than amorphous ones, a characteristic that was experimentally observed in previous studies (Göpferich and Langer, 1993a). The erosion of pixels is assumed to be a Poisson process. The lifetimes after contact with water were assumed to be distributed according to a first-order Erlang distribution (Drake, 1988):

$$e(t) = \lambda \cdot e^{-\lambda \cdot t}, \tag{1}$$

where λ is the erosion rate constant, which is different for crystalline (λ_c) and amorphous polymer (λ_a); $e(t)$ is the probability that a pixel will erode at time t after its first contact with water. Similar approaches for modeling Poisson processes with continuous time, but discrete space, have been used previously to model diffusion and reaction processes in zeolites (Tsikoyiannis and Wei, 1990).

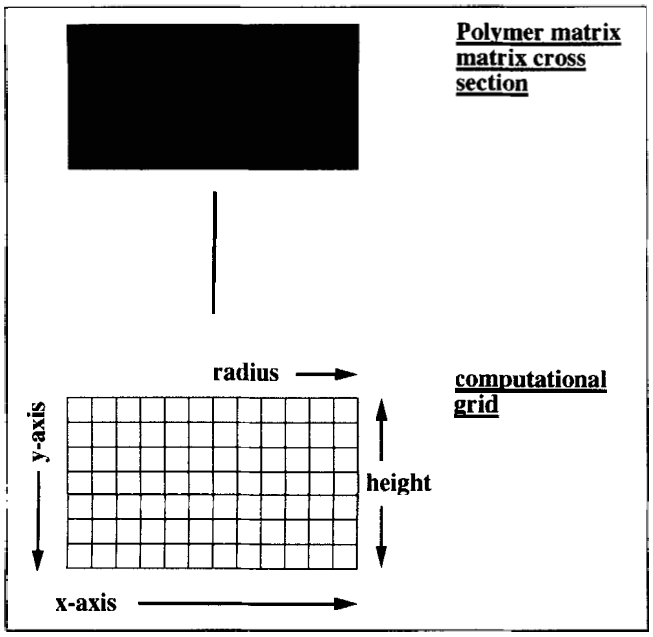

Figure 2. Polymer matrix representation by a computational grid.

This two-dimensional model cannot be used to describe the erosion of the three-dimensional cylinders. Several problems have to be solved to adapt it to describe erosion in three dimensions: cylinder cross sections have to be covered with a computational grid that takes the rotational symmetry into account; the ratio of radial stepsize to axial stepsize has to be found and erosion rate constants determined in previous studies have to be adjusted to the thicknesses of the new devices; and finally the coating has to be accounted for by choosing appropriate initial and boundary conditions.

Representation of the Cylindrical Cross Sections. First we represented cylinder cross sections by an appropriate computational grid, which is shown in Figure 2. Since the devices are rotationally symmetric, we used a modified two-dimensional grid instead of a three-dimensional one, which reduces the amount of necessary calculations substantially. It must be stressed, however, that this reduction of the dimensions is a substantial simplification. The definition of the stepsize in the x and y directions of the grid needs some circumspection. To define the stepsize of the grid, Δx, in the radial direction of the cylinders, we assumed that the lifetime of a pixel depends on its volume. If the stepsize in the horizontal direction, Δx, was constant as shown in Figure 2, the polymer volume represented by a pixel would depend on its radial position and increase while going from the inside of the cylinder to the outside.

The volume of a cylinder is proportional to the squared radius. If, therefore, the expansion of a pixel in the radial direction is a function of the root of the radius, r_i, as shown in Figure 3a, the pixels will represent a constant polymer volume.

Next we determined the ratio n_{xo} to n_y, the ratio of the number of grid points in radial and axial directions. This problem arises from the expansion of the grid in x and in y directions, thus enabling erosion to proceed from two directions. To make sure that erosion proceeds at the same speed from both directions, we assume that the step size Δy equals the step size Δx^2. Replacing Δy by the ratio of height, h, and number of pixels in the y direction, n_y, and Δx by the ratio of the squared total radius, r_o, and the pixels in the x direction, n_{xo}, we obtain

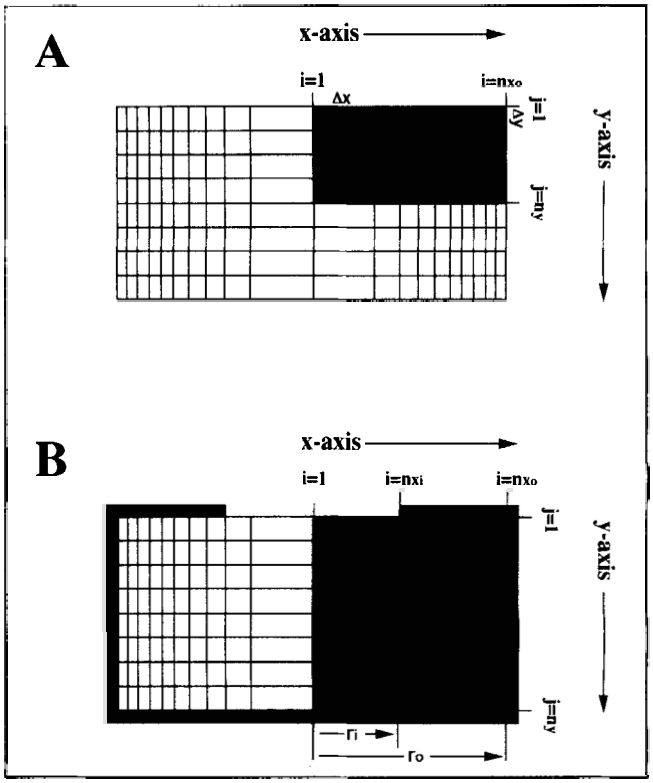

Figure 3. Computational grid for erosion simulation.
(a) Noncoated cylinder. (b) Coated cylinder.

$$\frac{h}{n_y} = \frac{r_o^2}{n_{xo}}. \tag{2}$$

Solving Eq. 2 for n_{xo} and n_y, respectively, we obtain

$$n_{xo} = \frac{r_o^2 \cdot n_y}{h}; \qquad n_y = \frac{h \cdot n_{xo}}{r_o^2} \tag{3a,b}$$

Equations 3a and 3b allow the calculation of either gridsize, n_{xo} and n_y when one of the two is fixed.

For partially coated cylinders we additionally had to define the ratio of pixels n_{xo} per total radius r_o to the number of pixels n_{xi} covering the orifice r_i. Assuming again that the number of pixels is proportional to the square of the total radius, we obtain

$$n_{xo} = \left(\frac{r_o}{r_i}\right)^2 \cdot n_{xi}; \qquad n_{xi} = \left(\frac{r_i}{r_o}\right)^2 \cdot n_{xo}. \tag{4a,b}$$

Setting Up the Computational Grid. The first step of modeling, setting up the computational grid, is shown in Figure

3a and 3b. Here we can take advantage of the rotational symmetry of the erosion problem. For the noncoated cylinder shown in Figure 3a, it is sufficient to take only a quarter of the cross section, which is represented by the shaded area, into account. For the partially coated cylinder shown in Figure 3b it is possible to reduce the problem to half of the cross section, again shown as a shaded area. This reduction decreases the amount of necessary calculations to 25% and 50%, respectively, of that of the original problem. The shaded pixels on the grid have first to be assigned an amorphous or crystalline quality. For reasons of simplicity we distributed the crystallinity randomly via Bernoulli trials:

$$c(x_{i,j}) = \begin{cases} 1-\chi & x_{i,j}=0 \\ \chi & x_{i,j}=1, \end{cases} \tag{5}$$

in which χ is the crystallinity of the polymer and $c(x_{i,j})$ is the probability of a pixel to represent an amorphous or crystalline part of polymer; $x_{i,j}$ represents the status of the polymer that can be crystalline ($x_{i,j}=1$), amorphous ($x_{i,j}=0$), or eroded ($x_{i,j}=-1$). For the subsequent simulations it is necessary to introduce a variable $s(x_{i,j})$, which describes the status of a pixel and distinguishes between eroded pixels ($s(x_{i,j})=0$) and noneroded pixels ($s(x_{i,j})=1$):

$$s(x_{i,j}) = \begin{cases} 0 & x_{i,j}=-1 \\ 1 & x_{i,j}=1 \\ 1 & x_{i,j}=0. \end{cases} \tag{6}$$

Next the boundary conditions had to be defined. Erosion proceeds from the surface of the polymer matrix that is exposed to the erosion medium. We therefore gave pixels on the surface fictive neighbors that are assigned the attribute "eroded" by setting their value as $x_{i,j}=-1$. This will initiate the erosion of pixels from the surface. We have to distinguish between coated and noncoated cylinders:

noncoated cylinders:

$$x_{i,j} = \begin{cases} -1 & 1 \le i \le n_{xo} \quad \text{and} \quad j=0 \\ -1 & i=n_{xo}+1 \quad \text{and} \quad 1 \le j \le n_y \end{cases} \tag{7}$$

coated cylinders:

$$x_{i,j} = -1 \qquad 1 \le i \le n_{xi} \quad \text{and} \quad j=0. \tag{8}$$

To account for the truncation of the complete grid to a reduced grid, reflection conditions are applied to the borders created by the cutting:

$$x_{i,j} = \begin{cases} x_{i,j-2} & 1 \le i \le n_{xo} \quad \text{and} \quad j=n_y+1 \\ x_{i+2,j} & i=-1 \quad \text{and} \quad 1 \le j \le n_y \end{cases} \tag{9}$$

Simulation of Erosion. For the simulation of erosion we used a Monte Carlo sampling technique that allows us to choose lifetimes at random from Eq. 1 (Cashwell and Everett, 1959; Kalos and Whitlock, 1986). Therefore, Eq. 1 is integrated and set equal to random variable ϵ, which is equally distributed between 0 and 1:

$$\Delta t_{i,j} = -\frac{1}{\lambda}\ln(1-\epsilon), \tag{10}$$

where $\Delta t_{i,j}$ is the lifetime of a pixel after its contact with the erosion medium. The algorithm proceeds by calculating the absolute lifetime $t_{i,j}$, which is the time gap between the start of the experiment and the "erosion" of a pixel $P_{i,j}$ according to the following scheme:

$$t_{i,j} = \begin{cases} \min t_{i,j} - \dfrac{1}{\lambda_a}\ln(1-\epsilon) & x_{i,j}=1 \quad \text{and} \quad \displaystyle\sum_{i-1}^{i+1}\sum_{j-1}^{j+1} s(x_{i,j}) < 9 \\ \min t_{i,j} - \dfrac{1}{\lambda_c}\ln(1-\epsilon) & x_{i,j}=0 \quad \text{and} \quad \displaystyle\sum_{i-1}^{i+1}\sum_{j-1}^{j+1} s(x_{i,j}) < 9 \\ t_{i,j} & x_{i,j}=-1 \quad \text{and} \quad \displaystyle\sum_{i-1}^{i+1}\sum_{j-1}^{j+1} s(x_{i,j}) < 9 \\ \infty & x_{i,j}\ne -1 \quad \text{and} \quad \displaystyle\sum_{i-1}^{i+1}\sum_{j-1}^{j+1} s(x_{i,j}) = 9. \end{cases} \tag{11}$$

The algorithm simulates erosion by repeatedly applying Eq. 11 to all pixels $P_{i,j}$ ($1 \le i \le n_{xo}$ and $1 \le j \le n_y$). After each of these runs the grid is searched for min $t_{i,j}$, which is the lifetime of the pixel that is next to erode. After each of these runs, $x_{i,j}$ and $s(x_{i,j})$ are updated. Equation 11 is applied in that way until the last pixel has been eroded.

Adjustment of Erosion Rate Constants. The only unknown parameters of the model are the erosion rate constants λ_a and λ_c. In a previous study we were able to determine these constants for crystalline and amorphous polymer areas (Göpferich and Langer, 1993b). To use them we first had to make them independent from the matrix thickness of the previous experiment. The easiest way these constants can

be adjusted is via the expected value of the Erlang function, $e(t)_{exp}$, for a pixel to erode, which is (Drake, 1988):

$$e(t)_{exp} = \frac{1}{\lambda}. \tag{12}$$

The time for an array of N pixels with the same λ value to erode from one end to the other is $N \times e(t)_{exp}$. To take the matrix thickness into account at constant N we have to assume that the expected value is proportional to the thickness of the matrix: that is, the thicker the matrix the more time will be needed to erode a single pixel. We obtain

$$\frac{e_{new}(t)_{exp}}{h_{new}} = \frac{e_{old}(t)_{exp}}{h_{old}}, \tag{13}$$

where subscripts old and new refer to the previously obtained and the calculated values. Substituting $1/\lambda_{old}$ for $e_{old}(t)_{exp}$ and $1/\lambda_{new}$ for $e_{new}(t)_{exp}$ in Eq. 13 and solving for λ_{new} yields

$$\lambda_{new} = \frac{h_{old} \cdot \lambda_{old}}{h_{new}}. \tag{14}$$

With the values determined previously (Göpferich and Langer, 1993b), Eq. 14 yields the erosion rate constants corrected for the new matrix thickness.

Simulations

After adapting the two-dimensional model to the three-dimensional erosion of cylinders, we used our model for simulations. First we examined cylinders that erode all over their surface, and investigated the effect of geometry on erosion. An erosion time series of a complete cylinder matrix cross section is shown in Figure 4. We used such simulations to determine the relative mass of eroded amorphous polymer, $m(t)$, which can be calculated from the grid during erosion:

$$m(t) = 1 - \frac{\sum_{i=1}^{i=n_{xo}} \sum_{j=1}^{j=n_y} s[x_{i,j}(t)] - x_{i,j}(t)}{(1-\chi) \cdot n_{xo} \cdot n_y} \quad \text{for } x_{i,j}(t) \neq -1. \tag{15}$$

Because the drug is located in the amorphous parts of the polymer, the amount of eroded amorphous polymer correlates with the amount of drug that is allowed to leave the implant. We assumed that a grid size of $n_y = 100$ would be sufficient. We found from two-dimensional studies that such grid sizes cause errors of less than 1% (Göpferich and Langer, 1993b). We assumed a fixed height of 1,000 μm and varied the ratio of radius to height between 0.5 and 1.7. The results of these simulations are shown in Figure 5.

From Figure 5 we can conclude that erosion depends markedly on the shape of the implant. This agrees well with models describing drug release from such implants (Göpferich and Langer, 1995b). The higher the ratio of radius to height, the more linear profiles are obtained, which was reported earlier (Hopfenberg, 1976; Cooney, 1972). Cylinders are completely eroded after 7 days, which is in agreement with the release profiles of monomers and indometacin from p(CPP-SA) 20:80 (Göpferich and Langer, 1995b).

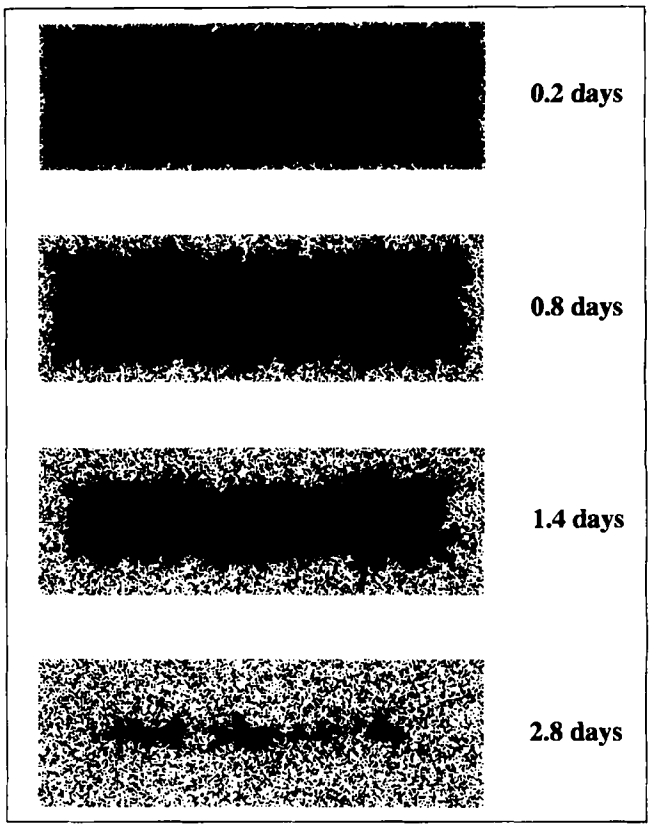

Figure 4. Erosion time series for a noncoated cylinder, complete cross section ($\chi = 0.35$, $n_x = 150$, $n_y = 100$, $\lambda_c = 8.75 \times 10^{-9}$ s^{-1}, $\lambda_a = 7.32 \times 10^{-7}$ s^{-1}, black pixels = noneroded polymer, white pixels = eroded polymer).

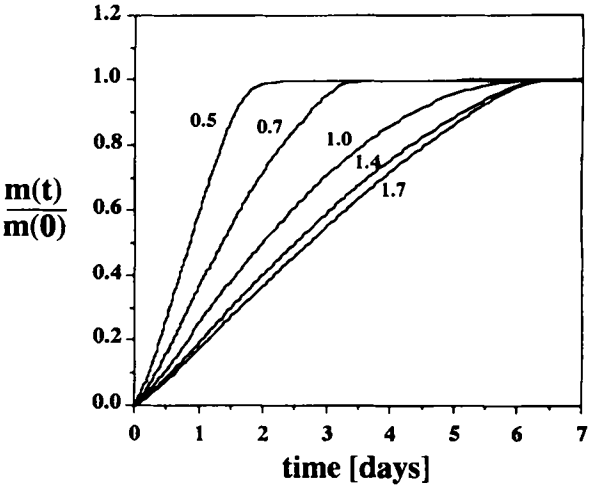

Figure 5. Influence of the ratio radius to height on the erosion of amorphous polymer areas ($n = 3$, $\chi = 0.35$, $h = 1{,}000$ μm, $n_y = 100$, $\lambda_c = 8.75 \times 10^{-9}$ s^{-1}, $\lambda_a = 7.32 \times 10^{-7}$ s^{-1}).

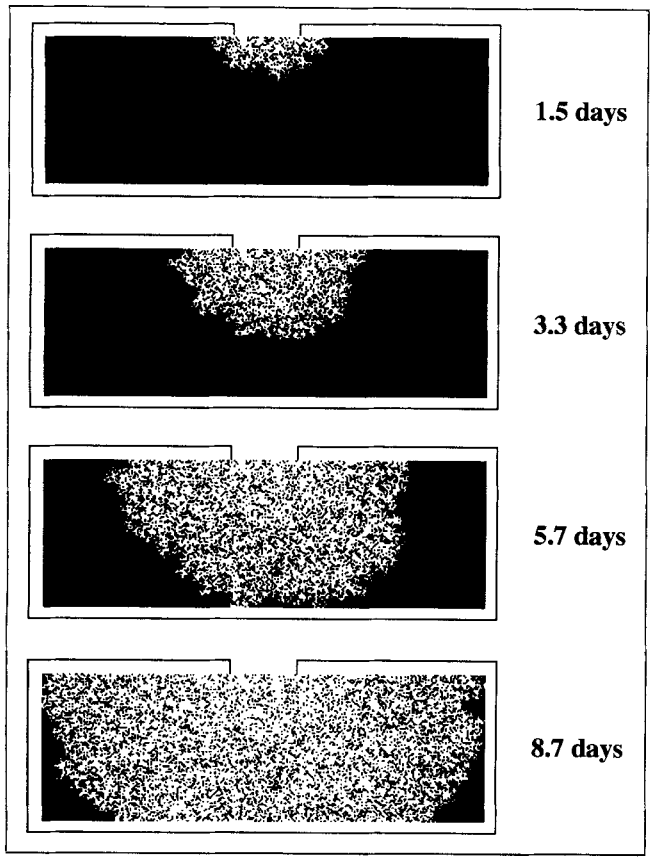

Figure 6. Erosion time series for a partially coated cylinder, complete cross section ($\chi = 0.35$, $n_{xi} = 50$, $n_{xo} = 150$, $n_y = 200$, $\lambda_c = 8.75 \times 10^{-9}$ s^{-1}, $\lambda_a = 7.32 \times 10^{-7}$ s^{-1}, black pixels = noneroded polymer, white pixels = eroded polymer).

We next wanted to investigate the benefit of coating implants, leaving just a small orifice on top of the noncoated implants. Figure 6 shows a time series of erosion simulations. The erosion of the implants starts on the surface exposed to the buffer and then moves deeper into the polymer. Erosion periods must be increased, as erosion fronts have to move longer distances to reach the walls of the matrix.

We next simulated the effect of varying the internal radius compared to the total radius. Figure 7 shows the effect on polyanhydride erosion. We varied the ratio of total radius to orifice radius between 1 and 2.8 while keeping the thickness of the disc constant. Figure 7 shows that erosion time periods can be expanded significantly if the cylinders erode from an orifice only. Depending on the geometry, erosion periods of several weeks can be achieved.

Prediction of Brilliant Blue Release from Noncoated Polymer Cylinders. There are many parameters of a polymer matrix disc that are affected by erosion. The samples lose weight and their porosity increases. Usually such changes would be good experimental indicators for erosion, but polyanhydrides tend to accumulate crystallized monomers inside pores (Göferich and Langer, 1993a), which alters both functions too much to obtain a good measure for erosion. An alternative is release profiles of substances that have low molecular weights

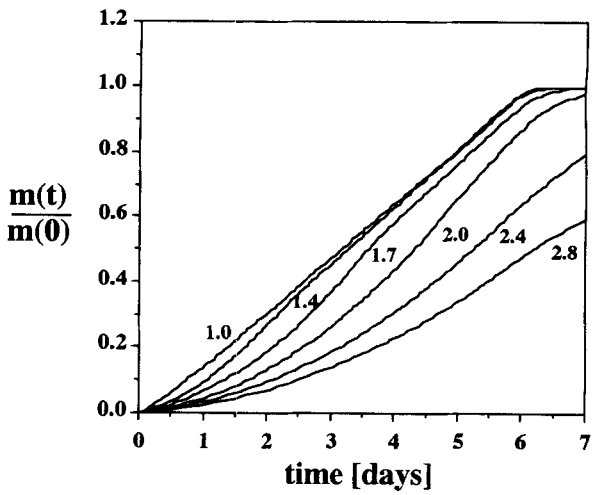

Figure 7. Influence of the ratio outer radius to inner radius on the erosion of amorphous polymer areas of a partially coated cylinder ($n = 3$, $\chi = 0.35$, $h = 1{,}000$ μm, $n_{xi} = 50$, $n_y = 200$, $\lambda_c = 8.75 \times 10^{-9}$ s^{-1}, $\lambda_a = 7.32 \times 10^{-7}$ s^{-1}).

from eroding polymer cylinders. These substances are trapped inside the matrix. Their release is triggered by erosion, which provides a network of pores leading to the surrounding buffer medium. There are many additional parameters that affect the velocity of drug and monomer release, such as diffusion or solubility. In the case of a highly water soluble compound, however, these effects are reduced to a minimum and the release velocity is controlled by the erosion velocity. In that case the erosion profiles match the release profiles. In Figure 8a and 8b the release profiles of brilliant blue are compared to the simulated erosion profiles. The agreement between the experimental release profile of the dye and the simulated erosion profile is reasonable. There are, however, significant deviations especially at early and later times of erosion. Since the drug is suspended, large amounts of drug located on the surface of the cylinder are released immediately after the start of the experiment. Therefore, the erosion profile is lower than the values of drug release. Toward the end of erosion, drug release is slowed significantly by the long diffusion pathway of drug from the inside of the disc to the surface. In general it can be concluded that the model predicts the erosion behavior of the cylinders without fitting any parameters.

Drug Release from Partially Coated Cylinders. To prove the benefit of coating for drug release, we coated 15% indomethacin loaded *p*(CPP-SA) 20:80 and *p*(FAD-SA) 50:50. As coating material we used D,L-PLA and EVAC. Figure 9 shows the release curves. These discs release the drug for twice as long as the noncoated systems. This difference is due to the protection of the cylinders against overall erosion as predicted by the Monte Carlo model. Besides erosion, diffusion of the drug through the coating might be possible. Drug release is, however, not very sensitive to diffusion effects, as the majority of the drug is released at a substantially decreased rate compared to noncoated systems. As shown in Figure 7, the release period can be further expanded by choosing an appropriate geometry and an appropriate orifice. An expansion of release periods will broaden the spectrum of applications for polyanhydrides significantly.

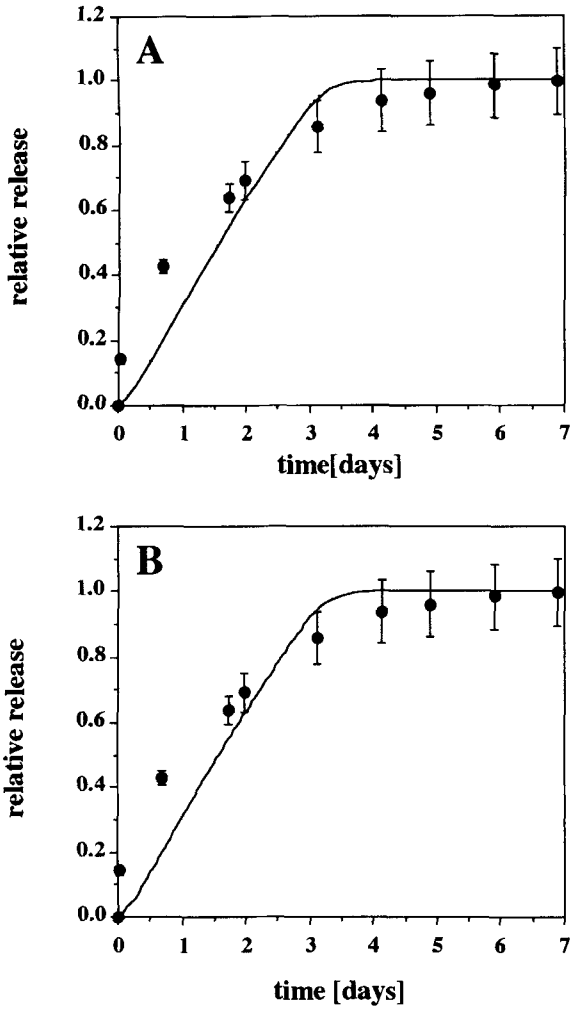

Figure 8. Model prediction of brilliant blue release from 5% loaded *p*(CPP-SA) 20:80 discs.

(A) r = 3,000 μm, h = 1,500 μm, χ = 0.35, n_y = 100, n_{xo} = 600, $\lambda_c = 5.8\times10^{-9}$ s^{-1}, $\lambda_a = 4.88\times10^{-7}$ s^{-1}. (B) r = 3,000 μm, h = 2,000 μm, χ = 0.35, n_y = 100, n_{xo} = 450, $\lambda_c = 4.4\times10^{-9}$ s^{-1}, $\lambda_a = 3.66\times10^{-7}$ s^{-1}.

Conclusions

The erosion of partially coated and noncoated polyanhydride cylinders can be predicted using a Monte Carlo model. The coating of devices allows the expansion of the period of drug release from 2 weeks to more than 5 weeks. This result makes polyanhydrides attractive candidates for therapies in an intermediate range of time.

Acknowledgments

Thanks are due to NATO and to the National Institutes of Health who sponsored this project by grants CRG 940721 and GM 26698. We thank Boehringer Ingelheim, Scios Nova, and Dupont for providing the polymers.

Notation

dx = radial step size
dy = axial step size
$E(t)$ = relative amount of amorphous polymer eroded at time t

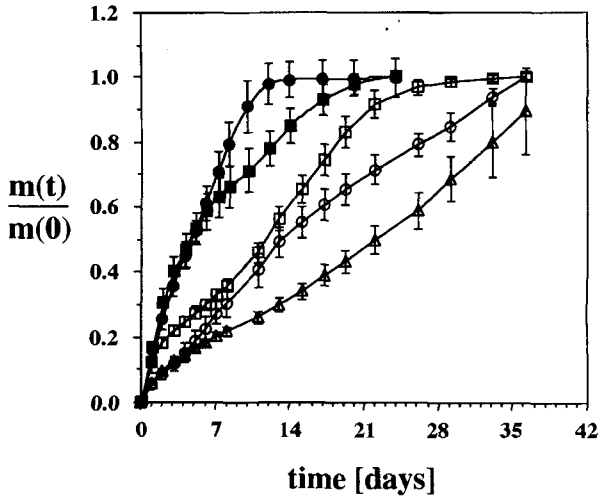

Figure 9. Indometacin release from coated polyanhydride.

■ *p*(FAD-SA) 50:50 noncoated (drug loading 5%); ● *p*(CPP-SA) 20:80 noncoated (drug loading 5%); □ *p*(FAD-SA) 50:50 coated with EVAC (drug loadinig 15%); ○ *p*(FAD-SA) 50:50 coated with D,L-PLA (drug loading 15%); △ *p*(CPP-SA) 20:80 coated with EVAC (drug loading 15%).

n = number of simulations
N = total number of pixels on the grid
$p(t)$ = erosion front position, μm
r = radius, μm
V = volume, cm^3

Literature Cited

Cashwell, E. D., and C. J. Everett, *A Practical Manual on the Monte Carlo Method for Random Walk Problems*, Pergamon Press, New York (1959).

Cooney, D. O., "Effects of Geometry on the Dissolution of Pharmaceutical Tablets and Other Solids: Surface Detachment Kinetics Controlling," *AIChE J.*, **18**(2), 446 (1972).

Drake, A. W., *Fundamentals of Applied Probability Theory*, McGraw-Hill, New York (1988).

Göpferich, A., and R. Langer, "The Influence of Microstructure and Monomer Properties on the Erosion Mechanism of a Class of Polyanhydrides," *J. Poly. Sci.*, **31**, 2445 (1993a).

Göpferich, A., and R. Langer, "Modeling Polymer Erosion," *Macromolecules*, **16**, 4105 (1993b).

Göpferich, A., R. Gref, R. Minamitake, L. Shieh, M.-J. Alonso, Y. Tabata, and R. Langer, "Drug Delivery from Bioerodible Polymers: Systematic and Intravenous Administration," in *Protein Formulations and Delivery*, J. Cleland and R. Langer, eds., ACS Symp. Ser. No. 567, Washington, DC, p. 242 (1994).

Göpferich, A., and R. Langer, "Modeling Monomer Release from Bioerodible Polymers," *J. Contr. Rel.*, **33**, 55 (1995a).

Göpferich, A., and R. Langer, "Predicting Drug Release from Cylindric Polyanhydride Matrix Discs," *Eur. J. Pharm. Biopharm.*, **41**(2), 81 (1995b).

Heller, J. "The Use of Poly(Ortho Esters) and Polyanhydrides in the Development of Peptide and Protein Delivery Systems," *Protein Formulations and Delivery*, J. Cleland and R. Langer, eds., ACS Symp. Ser. No. 567, Washington, DC, p. 292 (1994).

Herrmann, J. B., R. J. Kelly, and G. A. Higgins, "Polyglycolic Acid Sutures," *Arch. Surg.*, **100**, 486 (1970).

Hopfenberg, H. B., "Controlled Release from Erodible Slabs, Cylinders and Spheres," in *Controlled Release Polymeric Formulations*, D. R. Paul and F. W. Harris, eds., ACS Symposium Series No. 33, Washington, DC, p. 26 (1976).

Kalos, M. H., and P. A. Whitlock, *Monte Carlo Methods*, Wiley, New York (1986).

Langer, R., "Polymers for Sustained Release of Macromolecules: Their Use in a Single Step Method for Immunization," *Methods Enzymol.*, **73**, 57 (1981).

Langer, R., and N. Peppas, "Chemical and Physical Structure of Polymers as Carriers for Controlled Release of Bioactive Agents: A Review," *J. Macromol. Sci.-Rev. Macromol. Chem. Phys.*, **C23**, 61 (1983).

Langer, R., "New Methods of Drug Delivery," *Science*, **249**, 1527 (1990).

Rosen, H. G., J. Chang, G. E. Wnek, R. J. Linhardt, and R. Langer, "Bioerodible Polyanhydrides for Controlled Drug Delivery," *Biomaterials*, **4**, 131 (1983).

Rosen, H. B., J. Kohn, K. Leong, and R. Langer, "Bioerodible Polymers for Controlled Release Systems," *Controlled Release Systems: Fabrication Technology*, Vol. II, D. Hsieh, ed., CRC Press, Boca Raton, FL, p. 83 (1988).

Tamada, J., and R. Langer, "The Development of Polyanhydrides for Drug Delivery Applications, *J. Biomat. Sci. Poly. Ed.*, **3**(4), 315 (1992).

Tsikoyiannis, J. G., and J. Wei, "Diffusion and Reaction in High-Occupancy Zeolite Catalysts—II. A Stochastic Theory," *Chem. Eng. Sci.*, **46**, 233 (1992).

Wise, D. L., T. D. Fellman, J. E. Sanderson, and R. L. Wentworth, "Lactic/Glycolic Acid Polymers," *Drug Carriers in Biology and Medicine*, G. Gregoriadis, ed., Academic Press, New York, p. 237 (1979).

Zygourakis, K., "Development and Temporal Evolution of Erosion Fronts in Bioerodible Controlled Release Devices," *Chem. Eng. Sci.*, **45**(8), 2359 (1990).

Manuscript received Sept. 12, 1994, and revision received Dec. 3, 1994.